Title page

Title: Theory of visual attention thalamic model for visual short-term memory capacity and top-down control: Evidence from a thalamo-cortical structural connectivity analysis

Authors and Affiliations

Aurore Menegaux[1,2,3], Natan Napiorkowski[1,2,4], Julia Neitzel[1,5], Adriana L. Ruiz-Rizzo[1], Anders Petersen[6], Hermann J Müller[1,2], Christian Sorg[3,7 *], Kathrin Finke [1,2,4 *]

[1]Department of Psychology, General and Experimental Psychology, Ludwig-Maximilians-Universität München, Leopoldstrasse 13, 80802 Munich, Germany; [2]Graduate School of Systemic Neurosciences GSN, Ludwig-Maximilians-Universität, Großhaderner Strasse 2, 82152 Planegg, Germany; [3]Department of Neuroradiology, Klinikum rechts der Isar, Technische Universität München TUM, Ismaninger Strasse 22, 81675 Munich, Germany;[4]Department of Neurology, Jena University Hospital, Erlanger Allee 101, 07747 Jena, Germany; [5]Institute of Stroke and Dementia Research, Klinikum der Universität München, Feodor-Lynen-Straße 17, 81377 Munich, Germany; [6]Center for Visual Cognition, University of Copenhagen, Øster Farimagsgade 2A, Copenhagen, Denmark; [7]Department of Psychiatry, Klinikum rechts der Isar, Technische Universität München TUM, Ismaninger Strasse 22, 81675 Munich, Germany;

* These authors contributed equally

Corresponding author

Aurore Menegaux, Department of Psychology, General and Experimental Psychology, Ludwig-Maximilians-Universität München, Leopoldstrasse 13, 80802 Munich, Germany.

E-mail: aurore.menegaux@psy.lmu.de, phone: +49 89 2180 72567

Counts

Number of words: Abstract 218; Textbody 8304

Number of figures: 2

Number of tables: 2

Number of Supplementary material: 8

Abstract

In the theory of visual attention (TVA), it is suggested that objects in a visual scene compete for representation in a visual short-term memory (vSTM) store. The race towards the store is assumed to be biased by top-down controlled weighting of the objects according to their task relevance. Only objects that reach the store before its capacity limitation is reached are represented consciously in a given instant. TVA-based computational modelling of participants' performance in whole- and partial-report tasks permits independent parameters of individual efficiency of top-down control α and vSTM storage capacity K to be extracted. The neural interpretation of the TVA proposes recurrent loops between the posterior thalamus and posterior visual cortices to be relevant for generating attentional weights for competing objects and for maintaining selected objects in vSTM. Accordingly, we tested whether structural connectivity between posterior thalamus and occipital cortices (PT-OC) is associated with estimates of top-down control and vSTM capacity. We applied whole- and partial-report tasks and probabilistic tractography in a sample of 37 healthy adults. We found vSTM capacity K to be associated with left PT-OC structural connectivity and a trend-wise relation between top-down control α and right PT-OC structural connectivity. These findings support the assumption of the relevance of thalamic structures and their connections to visual cortex for top-down control and vSTM capacity.

Keywords: Diffusion tensor imaging, probabilistic tractography, neural theory of visual attention, visual short-term memory capacity, posterior thalamus

Abbreviations: vSTM, visual short-term memory; TVA, theory of visual attention; NTVA, neural theory of visual attention; DTI, diffusion tensor imaging; PT-OC, Posterior thalamus-occipital cortex; ROI, region of interest; IQ, intelligence quotient

Introduction

As our visual system is constantly confronted with more objects and features than it can process and consciously maintain simultaneously, selection is mandatory. To that end, the visual attention system distributes the limited resources in a way that allows preferential processing of relevant and filtering-out of irrelevant information (Desimone & Duncan, 1995). According to the 'theory of visual attention' (TVA; Bundesen 1990), visual processing is conceived as a parallel race between objects in a visual scene for representation in a visual short-term memory (vSTM) store that has a limited storage capacity (Bundesen, 1990). Only those objects that are selected into vSTM are consciously accessible, thus, available for voluntary, task-appropriate actions such as, e.g., verbal report. In line with the 'biased competition' account of attention (Desimone & Duncan, 1995), the competition for vSTM representation is assumed to be biased. According to TVA, the probability of a given object *x* to become represented in vSTM before its capacity limit is reached is proportional to the relative amount of attentional weight allocated to that object w_x compared to the weight of all other objects in the visual field. Besides bottom-up factors such as stimulus salience, the distribution of attentional weights across objects is influenced by top-down-controlled biases reflecting the objects' relevance to the current task goals.

Based on two simple psychophysical tasks involving verbal report of briefly presented letter arrays and TVA-based modelling, individual estimates of a given participant's efficiency of top-down controlled selection, parameter α, and vSTM capacity, parameter *K*, can be quantified. The individual efficiency of top-down control is derived from TVA-based fitting of performance in a 'partial-report task', in which participants have to name target letters (e.g., letters possessing a particular color) only while ignoring distractor letters (in a different color). Based on differences in report accuracy between conditions with and without distractors, separate attentional weights are estimated for target and distractor objects. The efficiency of top-down control, parameter α, is then derived as the weight allocated to distractors divided by the weight allocated to targets, w_D/w_T. The capacity of vSTM is derived from a 'whole-report task', more precisely, TVA-based fitting of the number of accurately reported letters from a letter array as a function of the (varying) effective exposure duration of the array (all letters are of the same color, so no selection is necessary in this task); formally, parameter *K* is estimated as the asymptotic value of the growth function relating report accuracy to exposure time. Typical estimates of vSTM storage capacity *K* in TVA-based paradigms in young healthy participants are around 3-4 items (e.g., Menegaux et al., 2017; Finke et al., 2005; Habekost 2015) which fits well with estimates obtained from other vSTM paradigms (Luck & Vogel 1997; Cowan, 2001; Vogel & Machizawa ,2004).

With respect to the underlying systems in the human brain, the neural interpretation of TVA (NTVA) suggests that 'visual' cortical regions, thalamic areas, and white-matter tracts interconnecting these regions are of particular relevance for top-down control and vSTM storage (Bundesen et al., 2005). In particular, it is assumed that, following a first, unselective wave of processing, attentional weights are computed for the displayed objects by a priority map in the pulvinar nucleus of the thalamus. In the subsequent, selective wave of processing, attentional weight signals from the pulvinar mediate biased processing of objects in visual brain areas, so that objects with higher attentional weights are processed, or represented by more neurons. The winners of the race are thought to be categorized in a vSTM map of locations assumed to be localized in the posterior thalamic reticular nucleus (see Figure 1). The reticular nucleus then gates activation in positive feedback loops that sustain the activity in neurons representing these winner objects. Thus, the NTVA model – in line with several authors suggesting a critical role of visual thalamic areas in the coordination of task-based attentional selection and vSTM (Bennaroch 2015; Danziger et al., 2001; Danzinger et al., 2004; Halassa & Kastner, 2017; Saalmann et al., 2012; Shipp et al., 2003; Shipp et al., 2004; Strumpf et al., 2013; Wurtz et al., 2011) – would predict that the structural connectivity between posterior thalamus and visual cortex is of relevance for both vSTM capacity and top-down control (Bundesen et al., 2005).

Empirical evidence for the relevance of these thalamic structures, i.e. the reticular nucleus and the pulvinar, and posterior white-matter connections for top-down controlled selection and vSTM storage is relatively sparse. The assumed role of the pulvinar for top-down control was supported by findings of impairments in task-based selection of targets among distractors and in patients with chronic pulvinar lesions (Snow et al., 2009). These results are similar to the inability to filter out irrelevant information in the visual field shown in monkeys following unilateral inactivation of the pulvinar (Desimone et al., 1989). Correspondingly, in neuroimaging studies, the pulvinar was found to be activated in paradigms requiring task-based selection of target among distractors (LaBerge et al., 1990; Nobre et al., 2002; Corbetta et al., 1991, Buchsbaum et al., 2006; Fischer & Whitney, 2012; Strumpf et al., 2013). With respect to vSTM capacity, Golestani and colleagues (Golestani et al., 2014) reported an association between vSTM span and white-matter microstructure of the optic radiations and the posterior thalamus. The first TVA-based study providing specific evidence for the presumed importance of thalamo-cortical tract structure for vSTM capacity comes from an analysis by Menegaux and colleagues (Menegaux et al., 2017). This study showed that in healthy young adults at the age of 26, a higher integrity of posterior thalamic radiations (as reflected by higher fractional anisotropy) was related to higher vSTM capacity. Nevertheless, no evidence for the presumed

association between the structural connectivity specifically of the posterior thalamus to visual cortices and vSTM capacity or top-down control of visual attention has been brought thus far.

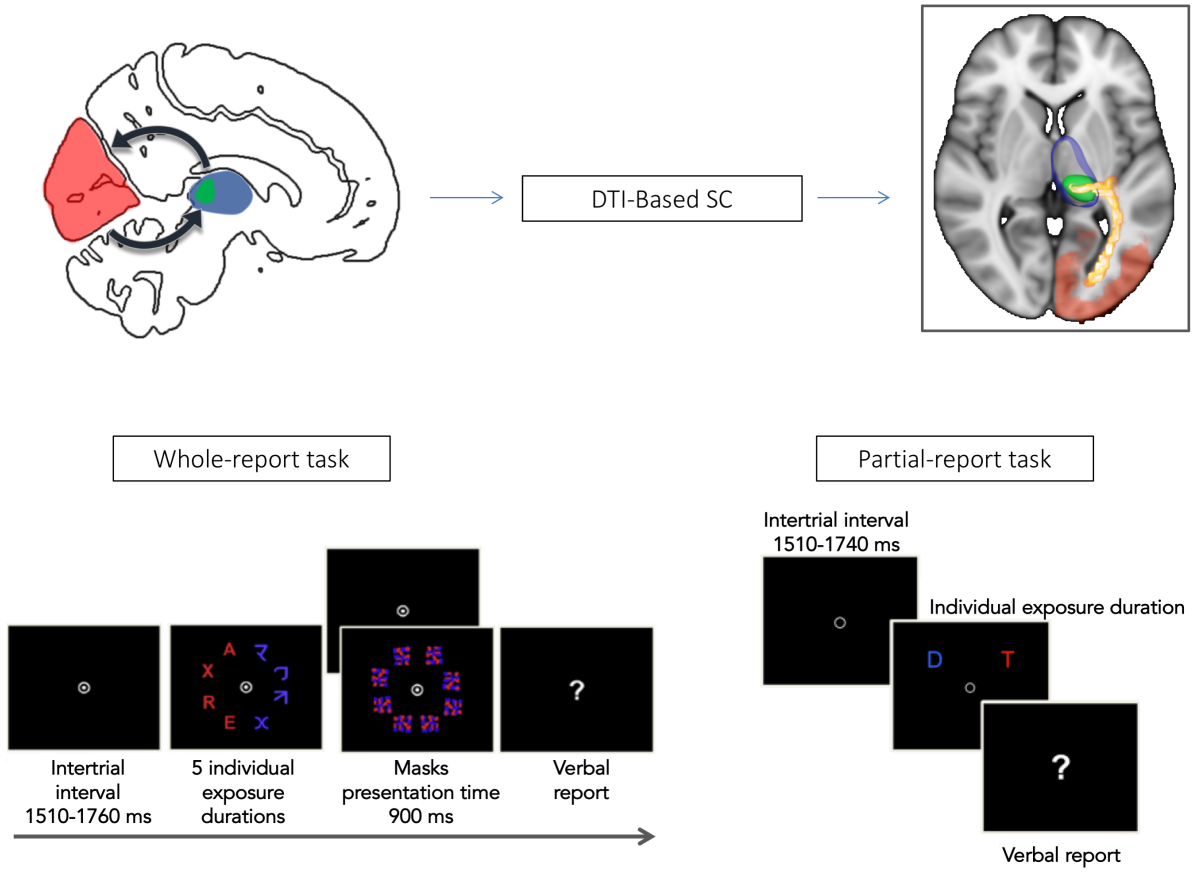

Figure 1: Presentation of the NTVA model, regions of interest (ROIs) and tasks used in this study. On the top left corner, the regions of interest derived from the NTVA model of Bundesen are shown with red representing the occipital cortex, blue the whole thalamus and green the posterior thalamus. On the top right corner an example of probabilistic tractography for one subject is represented; on the bottom left and right corner, representations of the whole and partial report tasks respectively are shown.

Based on the NTVA model assumptions on the importance of the posterior thalamus and of posterior thalamo-cortical communication for attentional prioritization of relevant information during visual processing and vSTM storage (Bundesen et al., 2005) and based on the prior evidence supporting this relevance (e.g., Fischer & Witney, 2012; Menegaux et al., 2017; Snow et al., 2009) we hypothesized that individual differences in structural connectivity of the posterior thalamus to occipital cortices (PT-OC) would be reflected in the efficiency of top-down control of attention as well as in vSTM capacity. In order to obtain an in-vivo measure of structural connectivity, we performed probabilistic PT-OC tractography, separately for each hemisphere. The score obtained from probabilistic

tractography indicates how frequently we can reconstruct a streamline between two points. In other words, it demonstrates how reproducible a pathway is (Jones 2010; Jones et al., 2013; Jeurissen et al., 2017). A higher number of streamlines associated with a voxel indicates a higher probability of a pathway to run through this voxel (Jones, 2010; Jones et al., 2013; Jbabdi & Johansen Berg 2011). Of note, this number of streamlines does not inform about the strength or quality of connections between those two regions. In other words, probabilistic tractography can only be used to test whether PT-OC connectivity is, in principle, associated with vSTM capacity *K* or top-down control α. However, it is difficult to make predictions concerning the direction of potential relationships (i.e., whether higher or lower connectivity would be related to better attentional performance). Probabilistic tractography was based on diffusion-weighted imaging data obtained from healthy individuals. The same subjects were assessed with TVA-based whole- and partial-report paradigms, in order to derive their individual vSTM capacity *K* and top down control α parameters, respectively. The association of these parameters with PT-OC connection probability was analyzed via partial correlation analysis, controlling for age, gender, crystallized IQ, and total intracranial volume (TIV). Left- and right-hemispheric PT-OC tracts were analyzed separately as their respective relevance for top-down control and vSTM capacity might differ. As, for example, in EEG and fMRI data pattern analyses the right compared to the left thalamo-cortical information transfer was found to be faster, it was suggested that the right-hemispheric system might be more relevant for fast selection of relevant stimuli and the left for their in-depth processing (e.g., Okon-Singer et al., 2011; see also Verleger et al., 2009, for similar conclusions). In more general terms, the right PT-OC tract might support a right-hemispheric dominance for attentional control (e.g. Fassbender et al, 2006; Hampshire et al., 2010; Garavan et al., 1999; Cieslik et al, 2015) while the left PT-OC might support a left-hemispheric dominance for object vSTM storage (Elliott and Dolan, 1998; Finke et al., 2006; Smith et al., 1995; Todd & Marois, 2005). In order to test the cognitively specific NTVA thalamic model of top-down control and vSTM storage (Bundesen et al., 2005; Habekost & Rostrup, 2007), control analyses were carried out on other TVA parameters that have been documented in prior studies to be related to white matter connectivity, although notably not specifically to PT-OC connectivity (Chechlacz et al., 2015; Habekost & Rostrup, 2007). Finally, in order to test our cortically specific assumption on the relevance of thalamo-occipital connections, control analyses were carried out on the structural connectivity between thalamus and motor cortex.

Material and methods

Participants

Thirty-seven participants, aged 21 to 53 years were included in the present study. All participants were fluent in German and had normal or corrected-to-normal vision. 32 participants were right-handed, 4 were left-handed, and 1 was ambidextrous according to the Edinburgh Handedness Inventory (Oldfield 1971). All the participants were highly educated, with years of school education ranging from 10 to 13 years (see Table 1) (M = 12.4 SD= 0.9). The German version of the multiple-choice vocabulary test MWT-B (Lehr, 1977) was used to measure crystallized IQ, and the Beck Depression Inventory test (BDI; Beck et al. 1996) was used to rule out depression.

	N = 37		
Variable	**Mean**	**SD**	**Range**
Gender (F/M)	22 / 15		
Handedness (R/L/B)	32 / 4 / 1		
Education (years)	12.4	0.88	10 - 13
Age (years)	33.8	10.54	20 - 53
K (elements)	3.31	0.54	2.37 - 3.88
C (elements/s)	24.7	8.66	12.02 - 47.01
T0 (ms)	10.73	11.74	0.0 - 49.0
α (a.u.)	0.43	0.14	0.17 - 0.67
W_{lat} (a.u.)	0.51	0.14	0.39 - 0.61
Crystallized IQ	95.8	15.0	72.5 - 140

Table 1: **Sample characteristics**

Exclusion criteria included alcohol intake at the day of testing, chronic eye diseases (e.g., colour blindness, glaucoma), history of neurological (e.g., brain injury, stroke) or psychiatric (e.g., anxiety disorder, schizophrenia) diseases, any occurrence of epileptic seizure, intake of medication affecting cognitive performance and claustrophobia. Additionally, participants with current symptoms of depression (BDI score > 18) were excluded as depression is known to alter visual top-down control (Desseilles et al., 2011) and thalamo-cortical functional connectivity (Brown et al., 2017).

50 participants were recruited for this study. In total, 13 participants had to be excluded: 3 because of high BDI scores, 4 because they did not follow the task instructions of the behavioral tasks adequately (3 in the whole-report and 1 in the partial-report task), 5 due to bad quality of and 1 due to incomplete diffusion-weighted imaging data. Our final cohort of participants consisted of 37 individuals. The study was approved by the ethics committees of the Department of Psychology of the Ludwig-Maximilians-Universität (LMU) Munich and the Medical Department of the Technische Universität München (TUM), and all participants gave prior informed consent in writing. Cognitive testing was performed at the LMU Department of Psychology, brain imaging at the TUM Department of Neuroradiology.

TVA-based behavioural assessment of vSTM capacity and top-down control

General assessment procedure

Whole- and partial-report tasks were conducted in a dimly-lit sound-attenuated chamber (Industrial Acoustics Company) with simultaneous EEG recordings[11]. Stimuli were presented to participants on a 24'' LED screen (800 x 600 pixel resolution, 100-Hz refresh rate) at a viewing distance of 65cm.

Each participant completed two sessions of 1.5 to 2 hours each on different days: in one session, the whole report was conducted and in another session the partial report task. Each session included EEG preparation, presentation of written instructions and stimuli used in the experiment, a procedure for adjustment of the individual exposure durations, and approximately 45 minutes of testing proper.

At the beginning of each trial, a fixation point (a white circle, 0.9° of visual angle in diameter, with a white dot in the centre) was presented in the centre of the display for a duration drawn randomly from 10 to 240 ms. Participants were instructed to fixate this marker throughout the blocks of trials administered. Following the fixation marker, red and/or blue letters were briefly presented on a black background. Letters' exposure durations were determined individually for each participant in a

[1]EEG recording was used for the assessment of event-related components (ERPs) during task performance, which are not the focus of the current study. Due to the special requirements of ERP investigation, some of the experimental trials in the whole- and partial-report tasks were repeated more often than others. Furthermore, for the ERP assessment, it was also necessary to ensure balanced visual stimulation in both hemifields in the whole-report task. This is why task-irrelevant (non-letter) symbols were presented in the visual hemifield opposite to the target stimuli. These specific manipulations, however, would not affect the TVA parameters derived from fitting report accuracy in the different conditions.

short pre-experimental practice session in order to ensure a comparable level of task difficulty across participants. The letters were randomly chosen from the following set {A, B, D, E, F, G, H, J, K, L, M, N, O, P, R, S, T, V, X, Z} and appeared only once in a given trial display. After stimulus presentation, a white question mark appeared in the centre of the screen, indicating the start of a verbal letter report. The participant could perform the report in any, arbitrary order, without speed constraint. In order to avoid too much guessing, participants were instructed to report only letters they were fairly certain they had seen. Following each block, participants received feedback related to the accuracy of the letters they actually reported (note that this feedback was independent from the overall performance level reached). A visual feedback bar indicated whether the report accuracy of the actually reported letters ranged between 70 and 90%. If accuracy fell below 70%, the participant was told by the experimenter to try to refrain from guessing and report only the letters they were relatively sure to have seen. If it was above 90%, the participant was encouraged to be less anxious and report more letters, even if not absolutely sure that they are correct. During the administration of both (the whole- and partial-report) tasks, the experimenter was seated behind the participant and entered the letters orally reported by the participant on a keyboard and then manually started the next trial by a key press action.

Whole-report task

On each trial, four letters were briefly presented along an imaginary semi-circle, of a radius of 5.27° of visual angle, either to the left or the right of the fixation point. Participants were instructed to report orally as many of the letters as possible. Four blue symbols (composed of random letter parts; see Figure 1) of the same luminance were displayed on the symmetrical semicircle on the other side of fixation. Letter and symbol stimuli subtended 1.3° of visual angle. At the beginning of each trial block, a white arrow in the center pointed towards the side on which the target (i.e., letter) stimuli would appear throughout the upcoming block. The target side in the first block was counterbalanced across participants and then alternated throughout the experiment. Seven timing conditions were used. In five conditions, the stimulus array was followed by post-display masks (see Figure 1) that consisted of eight red-blue scattered squares (also subtending 1.3° of visual angle) which were presented at each (letter and symbol) stimulus location for a duration of 900 ms. These arrays were presented for five different, individually adjusted exposure durations. In two additional conditions, the stimuli were presented unmasked, i.e., they were followed by a blank screen also presented for 900 ms. In one of these conditions, the exposure time was the second shortest duration (of the total five individually adjusted durations); in the other condition, the exposure time was fixed at 200 ms

for all participants. In these unmasked conditions, the exposure durations are effectively prolonged compared to the masked conditions, due to the uninterrupted visual persistence of the stimuli (Sperling, 1960). Thus, the five masked and the two unmasked conditions resulted in seven different effective exposure durations. The various experimental conditions were equally distributed across blocks of trials, and were displayed in randomized order within each block.

The exposure time adjustment phase consisted of 48 trials, divided into 4 blocks of 12 triples of trials. Each triple consisted of two trials that were not used for adjustment, but were simply presented for allowing the participant to become familiar with the task. These were either unmasked trials with an exposure duration of 200 ms or masked trials with an exposure duration of 250 ms. The critical trial display in each triple that was used for the exposure duration adjustment was masked and initially presented for 80 ms. Each time the participant reported at least one correct letter on this trial, exposure duration was decreased by 10 ms. When an exposure duration was reached at which the participant was no longer able to name a single letter correctly, this was set as lowest exposure duration used in the subsequent whole-report experiment proper. Based on this value, a set of 4 longer exposure durations was chosen from predefined sets.

The testing phase consisted of 10 experimental blocks, each of 40 trials. For each exposure duration, 30 trials were presented; the only exception was the condition with unmasked trials presented for 200 ms, for which 220 trials were presented (these were the critical trials for ERP analysis).

Partial-report task

On each trial, either a single (red) target letter, two target letters, or a target accompanied by a (blue) distractor were presented on a black background (see Figure 1). Red and blue letters were of the same luminance and had a size of 0.9° of visual angle. They appeared at the corners of an imaginary square, centred on the midpoint of the screen, with an edge length of 12.3° of visual angle. In displays containing two letters, these were presented either both vertically or both horizontally, but never diagonally.

Initially, 16 practice trials were presented with an exposure duration of 80 ms. Next, the procedure to adjust the individual exposure duration was applied, which consisted of 24 trials (4 single-target, 12 dual-target, and 8 target-distractor trials, in pseudorandomized order), with an initial exposure duration of 80 ms. Note that only the dual-target trials were used for exposure duration adjustment; the single-target and target-distractor trials were included simply to allow participants to become

familiar with all the conditions of the task. In the dual-target condition, if the participant reported both letters correctly, the exposure duration was decreased by 10 ms; if only one of the two letters was reported correctly, the exposure duration remained unchanged; and if none of the letters were reported correctly, the exposure duration was increased by 10 ms. Following this adjustment procedure, a performance check block with 24 trials (8 single-target, 8 dual-target, and 8 target-distractor-trials) was presented for the previously determined exposure duration. Accuracy for the single-target and the dual-target condition was displayed on the screen. The proper partial-report experiment was started by the experimenter when the accuracy achieved was within a range of 70 to 90% correct in the single-target condition and above 50% in the dual-target condition (i.e., if, on average, more than one letter was reported correctly in the dual-target condition). If performance was too high or too low, the exposure duration was manually adjusted by the experimenter, who also repeated the performance check procedure until an appropriate exposure duration was found. In total, 112 single-target, 112 dual-target, and 280 target-distractor trials were presented. Overall, there were 504 trials divided into 14 blocks. The experimental conditions were equally distributed across blocks, and were displayed in randomized order within the blocks.

Estimation of top down control and visual short term memory capacity

Modeling of participants' top-down control and vSTM capacity parameters utilized the TVA computational model implemented in the *lib*TVA toolbox for Matlab (Mads Dyrholm, www.machlea.com/mads/libtva.html). Detailed descriptions of the fitting procedure can be found in Dyrholm et al., 2011. In brief, top-down control was derived by modeling individual performance accuracy across the different partial-report conditions. This fitting procedure provided estimates of the attentional weights w_i assigned to both targets and distractors displayed at each location in the partial report experiment. Based on these values, the top-down control parameter (α), which reflects the difference in the weights assigned to targets w_T and distractors w_D, was estimated. As α is defined by the ratio w_D / w_T, (lower) α values approaching 0 indicate highly efficient top-down control, whereas values approaching 1 indicate rather non-selective processing. The spatial bias parameter w_{lat}, an indicator of the spatial distribution of attentional weights across the left (w_{left}) and right (w_{right}) visual hemifields, was also obtained from this fitting procedure. It is defined as the ratio w_{left} / (w_{left} + w_{right}). Thus, a value of w_{lat} = 0.5 indicates balanced weighting, a value of w_{lat} < 0.5 indicates a rightward spatial bias, and a value of w_{lat} > 0.5 indicates a leftward bias. The spatial bias parameter

w_{lat} was not of primary interest in our study, but was used to assess the cognitive specificity of our results[2].

Furthermore, vSTM capacity was derived by a TVA-based whole-report fitting procedure that models the probability of correct letter report in the whole-report as an exponential growth function with increasing (effective) exposure duration. The exposure time variation (7 durations) generated a broad range of performance which specified the whole probability distribution of the number of correctly reported elements as a function of the effective exposure duration. Parameter *K* is the asymptote of the fitted function, representing vSTM capacity in terms of the maximum number of items that can be simultaneously represented in vSTM[3]. The slope of the function at its origin represents visual processing speed (parameter *C*) which is defined as the rate of visual information uptake (in elements per second). Similarly to the spatial bias parameter w_{lat} in the partial-report task, the processing speed parameter *C* was drawn upon to ensure the cognitive specificity of our results. Two additional parameters which are of little or no interest for the questions at issue in the present study were also estimated: the perceptual threshold (parameter *t0*), the longest ineffective exposure duration (in ms) below which information uptake is effectively zero; and parameter μ, representing the prolongation of the effective exposure duration (in ms) on unmasked trials. For participants whose *t0* was estimated to be below 0 (4 out of 37), we refitted the data fixing *t0* at 0. This new fit did not modify the mean value of *K* and *C* parameters (Supplementary Table S1) nor any analyses in this study (Supplementary Table S2).

Imaging data acquisition

Whole brain T1- and diffusion-weighted imaging data were acquired on a 3T Philips Ingenia scanner with a 32 channel head coil and a SENSE factor of 2. Diffusion images were acquired using a single-shot spin-echo echo-planar imaging sequence, resulting in one non-diffusion weighted image (b = 0 s/mm^2) and 32 diffusion weighted images (b = 800 s/mm^2, 32 non-collinear gradient directions) covering whole brain with: echo time (TE) = 61 ms, repetition time (TR) = 14206.980 ms, flip angle =

[2] Finally, sensory effectiveness values for each hemi-field were obtained (A_{left} and A_{right}) that basically reflect how well stimuli were perceived, under the chosen exposure duration, in the left and the right hemi-field. This parameter is relevant for the valid estimation of top-down control and spatial attentional bias, but not relevant for the current study and not considered further.

[3] The *K* value reported is the expected *K* given a particular distribution of the probability that on a given trial *K* = 1,2,3, or 4 .

90°, field of view = 224 x 224 mm^2, matrix = 112 x 112, 60 transverse slices, voxel size = 2 x 2 x 2 mm^3. A whole head high-resolution T1-weighted anatomical volume was acquired using a 3D magnetization prepared rapid acquisition gradient echo sequence with the following parameters: repetition time = 9 ms; time to echo = 4 ms; inversion time, TI = 0 ms; flip angle = 8°; 170 sagittal slices; field of view = 240 x 240 mm2; matrix size = 240 × 240; reconstructed voxel size = 1 x 1 x 1 mm.

Quality check

All acquired MRI images were visually inspected by two independent raters (A.M., C.S.) for excessive head motion, and apparent or aberrant artifacts. In addition to visual inspection of the raw data, we also used the fitting residuals (the sum-of-squared-error maps generated by DTIFIT) to identify data corrupted by artifacts. Artifacts include motion-induced artifacts, insufficient fat suppression (ghosting) artifacts, and extreme distortion artifacts. Furthermore, fluid-attenuated inversion recovery-T2 images were acquired as part of the standard MRI protocol of the Klinikum Rechts der Isar and examined by experienced neuroradiologists to exclude potential lesions and white-matter abnormalities.

Preprocessing

Diffusion data preprocessing was performed using the FMRIB Diffusion Toolbox in the FSL software (www.fmrib.ox.ac.uk/fsl; Jenkinson et al., 2012) after converting data from DICOM to nifti format using mricron dcm2nii (Rorden et al., 2007) as described in previous work (Meng et al., 2015). All diffusion-weighted images were first corrected for eddy current and head motion by registration to the b0 image and skull and non-brain tissue were removed using the brain extraction tool (BET).

T1-weighted images were preprocessed using the anatomical processing script from FSL which included reorientation, image cropping, bias field correction, linear (FLIRT, FMRIB's Linear Image Registration Tool) and non-linear (FNIRT, FMRIB's Non-Linear Image Registration Tool) registration to MNI standard space. Output of this non-linear transformation included a structural-to-MNI standard space warp field and its inverse (MNI-to-structural). Anatomical preprocessing also included brain extraction (BET) and both tissue type and subcortical structure segmentations which were used to register diffusion weighted images to preprocessed structural T1-weighted images using boundary-based registration for echo planar imaging data thus yielding a diffusion-to-structural transformation

matrix. In order to register diffusion weighted data to the MNI 152 template via structural scan, we combined the previously generated structural-to-MNI non-linear transformation matrix with the diffusion_to_structural transformation matrix, thus resulting in a diffusion-to-standard space transformation. This transformation will be used later on to transform the individual fdt_paths, the 3D image file containing the output connectivity distribution to the seed mask, to standard space.

Probabilistic tractography and seed and target masks creation

Overall, we used several FSL atlases to define the occipital cortices, thalamic and exclusion masks for each hemisphere in standard space. Those masks were then transformed into native space using the previously described non-linear mapping, and probabilistic tractography was performed to identify the streamlines from occipital cortex to the thalamus within each hemisphere discarding inter-hemisphere estimates. The resulting path was then normalized and transformed into standard space, where a posterior thalamus mask for each hemisphere was used to extract the mean probability of connection value which was then correlated with the previously described attention parameters.

Regions of interest (ROIs) generation

We used the MNI 152 2-mm label atlas combined with the Harvard Oxford 2-mm cortical atlas to create our cortical occipital mask in standard space. Masks of the right and left thalamus were created from the Oxford thalamic 30% 2-mm connectivity atlas which is based on the probability of anatomical connections between the thalamus and the cortex in MNI space (Behrens et al., 2003). Additionally, whole brain left and right hemisphere masks were created from the Talairach atlas and used as exclusion masks in the tractography process. All masks were transformed into the subjects native space using the reverse non-linear mapping previously obtained and nearest neighbor interpolation.

Estimation of diffusion parameters and probabilistic tractography

Using the FDT toolbox from FSL, we first ran the function of Bayesian estimation of diffusion parameters obtained using sampling techniques (BedpostX) for each participant. It estimates the individual diffusion parameters at each voxel while automatically considering the number of crossing fibers per voxel (Behrens et al., 2003; Behrens et al.,2007). We used the default parameters

implemented in FDT: 2 fibers per voxel, weight of 1, and burning period 1000. Using the ROIs created as described above, tractography was run for each hemisphere with the occipital ROI as seed and the thalamus as waypoint target mask using the probtrackx2 function from FSL. We also used an exclusion mask from the opposite hemisphere in order to ensure the ipsilateral nature of the tractography. We performed tractography separately from each occipital ROI to the thalamus. For each participant, 5000 streamlines were initiated per seed voxel with a path length of 2000 × 0.5 mm steps, a curvature threshold of 80°, and loop checking criteria. The resulting image or fdt_paths represents the path connecting the seed region to the target, where the value in each voxel represents the number of streamlines generated from the seed region that pass through that voxel. Due to the differences in volume of each area across participants, we normalized the resulting tract estimates (fdt_paths) by dividing them by the waytotal (total number of streamlines generated from the seed region that reaches the target region) (Rilling et al., 2008), thus yielding a probability map of connectivity (Zhang et al. 2010, Arnold et al., 2012; Behrens et al.,2007; for review see Jbabdi et al., 2015). Those probability maps were then transformed back into standard space, so that they could be used for statistical analysis (Figure 1).

In order to assess the inter-individual variability of the thalamic probability maps, each individual probability map transformed into standard space was thresholded to exclude the lowest 20% of probability values voxels in order to reduce noise. Following this step, each individual's thresholded map was binarized and the mean of these maps was calculated. To visualize it, we thresholded this mean map to 0.9 to keep only voxels that were present in 90% of the individuals (supplementary material Figure S1 left). In a second step, we overlaid the posterior thalami masks, which revealed that most of its voxels overlapped with the mean map, indicative of a relatively stable connectivity pattern among participants (supplementary material Figure S1 right).

Estimation of total intracranial volume (TIV)

In order to obtain volumetric measurements for the whole brain, T1 images were segmented into grey matter, white matter and cerebrospinal fluid tissue classes and normalized to the MNI 152 mm template using DARTEL (SPM12 software package, http://www.fil.ion.ucl.ac.uk). The segmented and normalized images were modulated to account for the structural changes resulting from the normalization process, thus indicating grey matter, white matter and cerebrospinal fluid volume. A measure of total intracranial volume was estimated by first computing and then adding up the totals

(in liters) of the warped, modulated, and unsmoothed grey-matter, white-matter and cerebrospinal-fluid segments with the in-built SPM Tissue Volumes Utility (Malone et al., 2015).

Statistical analyses

For each individual connection probability map, posterior thalamus masks of each hemisphere were used to extract the mean probability of connection from these regions. A posterior thalamus mask was created for each hemisphere using the Talairach labels 2mm atlas, which, owing to the low resolution of MRI, contained the thalamic reticular nucleus as well as the pulvinar nucleus. Since normal distribution was not confirmed for all variables (via Kolmogorov-Smirnov test), Spearman partial correlation was used to assess the association among left and right PT-OC connection probability and top down control/vSTM capacity. In order to investigate these associations further, we performed multiple linear regression analyses with vSTM capacity or top-down control as dependent variable and left or right PT-OC connection probability as independent variable, respectively. For all correlations and regressions, gender, handedness, age, crystallized IQ, and TIV were included in the model in order to control for these effects of no interest. All analyses were performed using the SPSS statistics package version 21 (IBM).

Control analyses

In order to test the structural specificity of our connectivity results for the occipital region, we performed tractography from the motor cortex as control ROI to the thalamus. We used Brodmann areas 4a, 4p, and B6 from the Jülich atlas, separately for each hemisphere, combined with the Harvard-Oxford 2-mm cortical atlas to create the cortical motor masks for the left and the right hemisphere. Similarly, the Harvard-Oxford 2-mm cortical atlas combined with the MNI 152 2-mm label atlas were used to create left and right parietal cortex masks. Furthermore, in order to test the cognitive specificity of our results for vSTM capacity K and top-down control α, the TVA parameters processing speed C and spatial bias w_{lat} were correlated with left and right PT-OC connection probability using Spearman partial correlation.

Results

Behavioural data

The mean vSTM storage capacity *K* value of our sample was 3.31 (SD = 0.39) (see Table 1), and the mean top down control *α* value was 0.44 (SD = 0.14), consistent with highly similar previous findings in healthy participants (e.g., Finke et al., 2005; Kraft et al., 2015). Moreover, in line with the assumption of the TVA model (Bundesen 1990) that the two parameters reflect independent attentional functions, vSTM capacity and top down control were not significantly correlated with each other ($r_s(35) = 0.28$; p = .10).

PT-OC structural connectivity and vSTM capacity

In order to test our hypothesis that PT-OC connection probability would be significantly associated with vSTM capacity, we performed two separate Spearman correlation analyses between PT-OC connection probability obtained from tractography for the left and the right hemisphere and *K*, controlling for gender, age, handedness, IQ, and TIV. We found the left hemisphere PT-OC connection probability to be significantly negatively associated with *K* ($r_s(30) = -0.38$; $p = .03$). The relevance of left PT-OC connection probability for vSTM capacity was further confirmed using a multiple linear regression model. We found that left PT-OC connection probability was significantly associated with vSTM capacity (β = -26.823; p = .008; Table S3). This association remained significant after Bonferroni correction (p <0.0125).

However, no significant association between *K* and the right hemisphere PT-OC connection probability was found ($r_s(30) = 0.02$; $p = .91$; Figure 2 and Table 2). This lack of significance was further confirmed via multiple linear regression where right PT-OC connection probability did not significantly link with vSTM capacity (β = -3.605; p = .78; Table S4).

PT-OC structural connectivity and attentional selection

In order to test our hypothesis that PT-OC connection probability would be associated with top-down control, we performed separate Spearman correlation analyses between PT-OC connection probability obtained from tractography for the left and the right hemisphere and top-down control *α*, again controlling for gender, age, handedness, IQ, and TIV. We observed a trend for a significant

positive correlation between α and right PT-OC connection probability ($r_s(30) = 0.31$; $p = .08$), that is: higher connectivity between posterior thalamus and occipital cortices tends to be related with less efficient top-down control. Using a multiple linear regression model, we found that right PT-OC connection probability was associated with top-down control (β = 8.85; p = .046; Table S6). However, this association did not survive multiple comparison correction. We did not find any association between left PT-OC structural connectivity and α ($r_s(30) = -0.06$; $p = .74$; Figure 2 and Table 2) which was further confirmed using multiple linear regression where left PT-OC connection probability was not significantly linked with top-down control (β = -1.232; p = .752; Table S5).

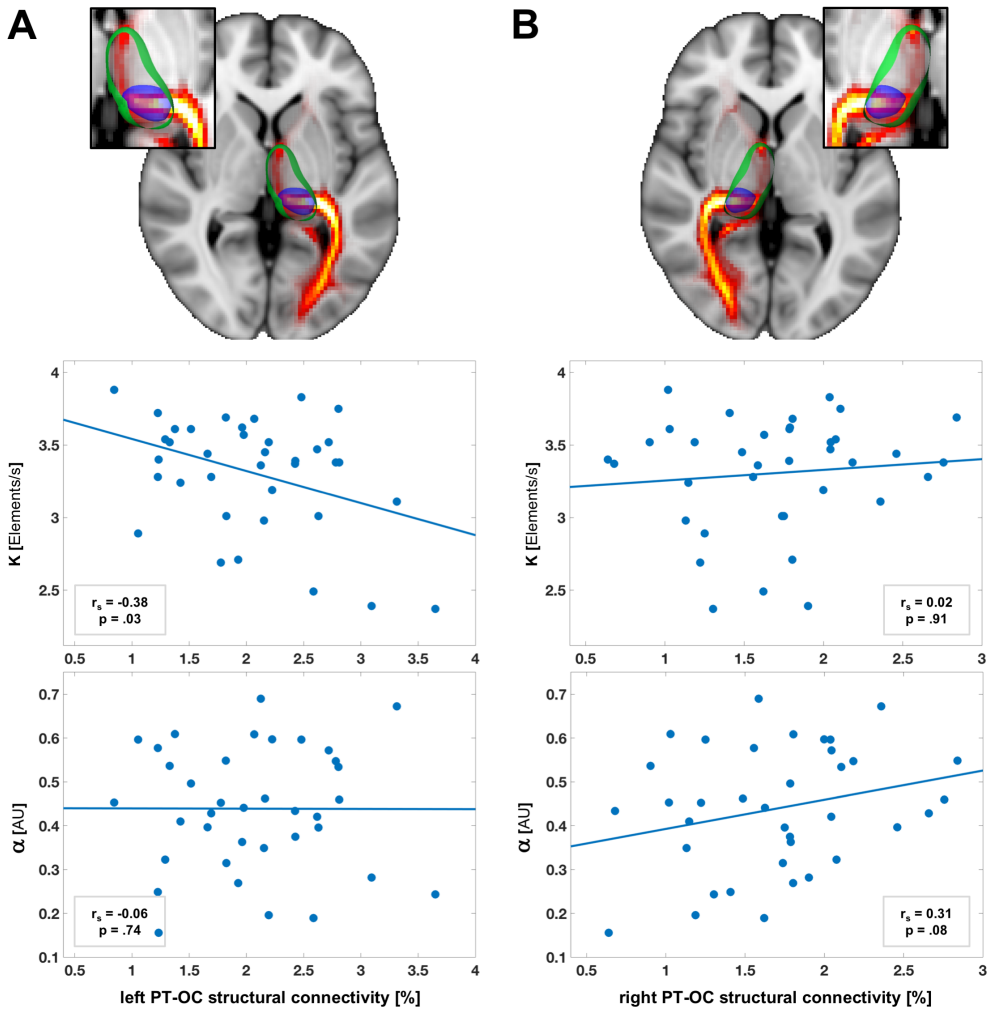

Figure 2: Structural connectivity between posterior thalamus and occipital cortices is associated with vSTM capacity and top down control. The first row illustrates probabilistic tractography between occipital cortices and left (**A**) or right (**B**) thalamus respectively. Green represents left and right thalamic masks and blue left and right posterior thalamic masks. The second and third rows show graphs representing vSTM capacity and top down control respectively, as a function of left or right structural connectivity. Data points were correlated by Spearman correlation with correlation coefficient r_s and significance level p. The lines in the graphs represent linear regression lines, for illustration.

Control analyses[4]

Analyses of cortical specificity: vSTM capacity and top down control are not associated with posterior thalamus-motor cortex structural connectivity

In order to test the cortical specificity of the association between PT-OC structural connectivity and vSTM capacity, we investigated whether the parameters vSTM storage capacity and/or top-down control would also be associated with structural connectivity of the posterior thalamus with regions not supposed to be relevant for top-down control or visual short-term maintenance, i.e., with the left and the right motor cortex. We did not find any significant associations (highest r_s-value: 0.23; lowest *p*-value: .22; Table 2).

Analyses of functional specificity: PT-OC structural connectivity is not associated with processing speed or spatial bias

In order to test whether the results obtained for vSTM storage capacity *K* and top-down control were cognitively specific, we additionally correlated left- and right-hemisphere PT-OC connection probability with the TVA parameters visual processing speed *C* and spatial bias w_{lat}, via Spearman partial correlations. We did not find any significant correlations (highest r_s-value: 0.24; lowest *p*-value: .19; Table 2).

[4] As one reviewer suggested that, in order to retrieve critical information on a potential functional hemispheric specialisation of PT-OC tracts, the analyses should include those of the role of lateralization of fiber tracts , we investigated the association between vSTM capacity and top-down control and a tract lateralization index ($PT\text{-}OC_{left} - PT\text{-}OC_{right}/(PT\text{-}OC_{left}+PT\text{-}OC_{right})$). As the role of tract lateralization was beyond the scope of our study, we display these correlation results in table S7 in supplementary material. Both vSTM capacity *K* and top-down control α showed a significant inverse correlation to the tract lateralization index. As the effect size of these correlation are of similar magnitude as those obtained from the unilateral analyses (left PT-OC and vSTM capacity *K*; right PT-OC and top-down control α) we assume that the correlation to the lateralization index rather reflects the unilateral significant relationship of the respective fiber tracts to the attentional parameters.

		Test ROIs		*Control ROIs*	
		Left PT-OC SC	**Right PT-OC SC**	**Left PT-MC SC**	**Right PT-MC SC**
Test variables	***K***	**r = -0.38 p = .03***	r = 0.02 p = .91	r = 0.03 p = .80	r = -0.10 p = .59
	α	r = -0.06 p = .74	**r = 0.31 p = .08**	r = 0.01 p = .99	r = -0.23 p = .22
Control variables	***C***	r = -0.17 p = .36	r = 0.09 p = .64	r = 0.09 p = .62	r = -0.01 p = .96
	w_{lat}	r = 0.24 p = .19	r = 0.13 p = .50	r = 0.27 p = .14	r = 0.12 p = .50

Table 2: Correlation between TVA parameters and posterior thalamus structural connectivity.
Abbreviations**:** PT-OC: Posterior thalamus to occipital cortex; PT-MC: Posterior thalamus to motor cortex; SC structural connectivity. ROI: Region of interest. Correlations below p = .10 are shown in bold, * indicates p < .05.

Discussion

According to the NTVA model (Bundesen et al., 2005), the pulvinar nucleus of the thalamus contains the priority map of objects where attentional weights are computed and bias the processing of objects in visual brain areas. Based on this assumption, we investigated whether PT-OC structural connectivity was associated with top-down control in healthy individuals. Furthermore, the NTVA model suggests that posterior thalamic nuclei and, in particular, the TRN are relevant for vSTM capacity by sustaining the activity of visual cortical neurons representing the objects through a feedback loop. Accordingly, we also investigated whether PT-OC structural connectivity was associated with vSTM capacity in healthy individuals.

We found evidence for the relevance of fiber tracts connecting the posterior thalamus and the visual cortex areas for both of these functions. In more detail, we observed a non-significant trend for estimates of top-down control α to be related to the probability of connection between the right posterior thalamus and the right occipital cortex. Furthermore, the individual estimates of vSTM capacity were significantly inversely related to the probability of connection between the left posterior thalamus and the left occipital cortex. These associations were structurally specific to the occipital cortex, as the probabilities of connections between the thalamus and motor cortex did not show the respective associations. Furthermore, they were also cognitively specific, as control analyses for other visual attention functions (visual processing speed C and spatial bias w_{lat}) did not show respective relationships.

Thus, our results suggest that the PT-OC fiber tracts might indeed serve specific roles in task-related top-down control and short-term maintenance, as assumed in the NTVA model, rather than playing a more general, broad role in diverse attention functions.

The relevance of PT-OC structural connectivity for top-down control

We found a trend-to-significance relation between the individual level of top-down control α and the right PT-OC connectivity. Although this finding cannot be taken as strong empirical evidence for the NTVA due to the lack of statistical significance, it is in line with the assumption that the pulvinar is relevant for top-down control. As in NTVA it is assumed that, following the computation of attentional weights of the objects in the visual display, the pulvinar transmits weighted information to higher-order visual areas (Bundesen et al., 2005); it follows that the connection between posterior

thalamic areas and the occipital cortex would be relevant for the efficiency of task-related prioritization of relevant objects. The lack of significance in our young healthy sample might be related to a reduced variability and lack of statistical power. It is to be expected that more clear relationships would be found in analyses of pathological systems. Indeed, consequences of experimental lesions to the pulvinar in monkeys (Desimone et al., 1989) and respective acquired damage in humans (Snow et al., 2009) on task-based selection have been reported. Snow and colleagues found deficits in discriminating target features when in the presence of salient distractors – suggesting a role of the pulvinar in task-based competition of objects for selection, as assumed by NTVA. It is to note that TVA-based analyses of the consequences of pulvinar lesions did not report such deficits. However, as such patients are rare; these are limited to single case reports (Kraft et al., 2015; Habekost and Rostrup, 2006). Thus, based on our results, a relevant future question would be whether pathological changes in (right-sided) PT-OC connectivity are related to deficits in top-down control. Our findings also fit to those of neuroimaging studies that repeatedly reported enhanced pulvinar activation during task-based selection (LaBerge et al., 1990; Nobre et al., 2002; Corbetta et al., 1991; Fischer & Whitney, 2012; Strumpf et al., 2013).

The finding that the trend-to-significance relationship is only found for the right (and not the left) PT-OC structural connectivity can be related to findings of Okon-Singer et al. (2011) who, using dynamic causal modeling, demonstrated that thalamo-cortical information transfer is faster within the right than within the left hemisphere. As event-related EEG potentials indicating target selection in the face of distracting information also have earlier and larger amplitudes of peaks at right compared to left-sided electrodes (Verleger et al., 2009), Okon-Singer et al. (2011) assumed that especially information transfer between right thalamus and posterior cortex structures is relevant for efficient target selection processes according to task goals. On a more general level, our finding adds support to the assumption of a hemispheric specialization of a right-hemispheric network for visual attentional top-down control (e.g. Fassbender et al., 2006; Hampshire et al., 2010; Garavan et al., 1999; Cieslik et al, 2015). Furthermore, it indicates that visual attentional top-down control is supported by thalamo-cortical information transfer.

PT-OC structural connectivity is associated with vSTM capacity

Our finding of a significant association between vSTM capacity and left PT-OC connection probability is in line with the NTVA assumption of recurrent loops between posterior thalamus, and more specifically: the reticular nucleus, and visual cortices subserving reactivation and maintenance of

selected visual object information (Bundesen 2005). In TVA, visual processing is conceived as a race between objects for representation in capacity-limited vSTM (Bundesen 1990). The objects that win the race are thought to be categorized in a vSTM map of locations situated in the posterior thalamus, more precisely: the TRN (Bundesen 2005). In consonance with Hebb (1949), for example, the NTVA suggests that in visual cortices, the activity of the neurons representing the winning objects is sustained and reactivated by a feedback loop gated by the TRN. Our findings go beyond previous TVA-based studies that revealed an association between microstructure in posterior white matter and vSTM capacity (Habekost and Rostrup 2007, Espeseth et al., 2014), in that they provide structurally more precise evidence for the importance of especially the connection between posterior thalamus and occipital cortex. In this regard, our findings further confirm the role of the tracts connecting the posterior thalamus to visual cortices for vSTM capacity, which was suggested in a previous study by Menegaux et al. (2017). Our findings are complementary to those of Golestani and colleagues, who found the microstructure of the posterior thalamic radiations as well as other posterior thalamic tracts, the optic radiations, to be relevant for individual vSTM capacity (Golestani et al., 2014).

The finding of a negative association between vSTM capacity and left PT-OC structural connectivity shows that vSTM capacity is associated with a characteristic of this pathway. Due to the largely unknown basis of the probability of connection value, it is not possible to identify the precise characteristic that renders the relation between the connectivity value and VSTM capacity. Indeed, the probability of connection between the occipital cortex and the posterior thalamus reflects the number of streamlines connecting those two ROIs. As the number of streamlines is not a direct measure of anatomical connectivity and as their relationship to the underlying anatomy is unclear (Jones et al., 2013; Jbabdi & Johansen-Berg, 2011), lower connectivity values do not necessarily indicate lower strength of connection or fewer axons between PT and OC. Furthermore, it is important to note that here we use the term ‘probability of connection’ to refer to the probabilistic tractography score obtained by probtrackx. As explained by Jones and colleagues who prefer the term ‘stochastic tractography score’, the tractography score indicates how frequently a streamline between two points can be reconstructed, and there are many reasons why a streamline might not be successfully reconstructed (Jones et al., 2013). Differences in ‘true’ connection strength is one of them (Jones et al., 2010). Indeed, several factors can influence the number of streamlines such as the organization of myelin in regions bordering cortical grey matter (Reveley et al., 2015) as well as fanning fibers or crossing fibers. For example, fewer crossing fibers would yield increased connectivity values (Jbabdi & Johansen-Berg 2011; Thomas et al 2014; Reveley et al., 2015; Donahue et al., 2016). Dense white-matter fiber bundles at the grey matter/white matter boundary would

impede tractography detection of weaker crossing fibers entering or exiting grey matter in sulcal fundi and thus influence the number of streamlines. This also applies to inter-individual differences in axon diameter distribution as well as the distance between the two regions of interest (Donahue 2016; probably Thomas, 2014; Behrens 2007). Considering the complex meaning of the probability of connection value obtained from probtrackx, our results can be taken to suggest that both vSTM capacity and, to a lesser extent, top-down control depend on the path between posterior thalamus and occipital cortex. However, the nature of the association, i.e., the precise underlying characteristics of the tracts that are related to the attention functions can only be revealed in further investigation. These could use, for example, diffusion MRI methods that can resolve intravoxel structure such as high angular resolution diffusion imaging (Tuch et al., 2002; Tuch et al., 2003).

The fact that the left, and not the right, PT-OC connection probability was found to be related to vSTM might be an indicator of a more relevant role of the left hemisphere for vSTM storage of object information. This might indicate that the vSTM feedback loop, in young healthy participants, mainly relies on left-sided thalamo-cortical connections, maybe reflecting a prominent role of a left-hemispheric system for vSTM storage. This is in line with a previous PET study analyzing the respective relevance of the two hemispheres in visual-spatial vs. visual- object short-term storage with structurally equivalent tasks (Smith et al., 1995). The results implied that, while a right-hemispheric system seem to be specialized in vSTM for spatial information (see also Awh & Jonides, 2001), a left-hemispheric system appeared to be specialized in object information. Furthermore, using fMRI, Todd & Marois (2005), found that left-sided parietal activation predicted the individual level of vSTM capacity. Finally, also analyses of the consequences of unilateral posterior parietal damage in humans indicated that a left-sided vSTM system might be specialized for the maintenance of visual object information (Finke et al., 2006). Together with such PET, fMRI and patient data, our results imply that, at least in young healthy participants, particularly the PT-OC communication within the left hemisphere might support the vSTM loop activation proposed in NTVA (Bundesen et al., 2005).

Limitations

The present study has several limitations. As the sample consisted of relatively highly educated participants, the results might be impacted by a selection bias. This might have led to reduced variance in cognitive and structural measures and thus an underestimation of correlations that would

be found in a less selective sample. Another limitation lies in the relatively small number of participants involved. Additional limitations include inherent tractography difficulties, such as the unknown directionality of connections (as pointed out above), the influence of distance on tractography, and false positive results of anatomical connections owing to various physical and biological factors (Thomas et al., 2014). Moreover, it has been shown that partial volume effect can affect tractography (Vos et al., 2011). Thus, the present results should be considered with care. Finally, in contrast to *K* which was found to be the most reliable TVA parameter, it was found that top-down control parameter α has a relatively low re-test validity when measured with a shorter combi-TVA task with partial and whole report trials (Habekost et al., 2014). Thus, the non-significant trend of an association between top-down control and right PT-OC connection probability should be regarded with more caution and future studies might not be able to replicate this finding. Note, however, that the longer partial report task used in this study is more homogenous with respect to display types and includes more trials which should make the top-down control measure more reliable as indicated by Finke et al., (2005). Finally, we used a large ROI for the occipital region, which does not allow us to say which specific area of the occipital lobe is linked to the attentional measures.

Conclusion

We investigated whether the structural connectivity of posterior thalamus to occipital cortices is associated with vSTM capacity and top-down control of attention selection as suggested by the NTVA model. We found that vSTM capacity was significantly associated with structural connectivity of left posterior thalamus to occipital cortex, and a trend towards an association between the structural connectivity of right posterior thalamus to occipital cortex and top-down control. These findings constitute the first evidence in support of the assumption that thalamic structures and their connections to visual cortex are of relevance for both top-down control and vSTM capacity.

Acknowledgments

We thank Erika Künstler and Annette Abraham for their help with both the recruitment of participants, and the collection of TVA data. We are grateful to the staff of the Department of Neuroradiology in Munich particularly Dr. Christine Preibisch and Stephan Kaczmarz for showing us how to operate the scanner. Most importantly, we thank all our participants for their efforts to take

part in this study. This study was supported by EU Marie Curie Training Network INDIREA (ITN- 2013-606901 to H.J.M., and K.F.), Deutsche Forschungsgemeinschaft (FI 1424/2-1 to K.F. and SO 1336/1-1 to C.S.), German Federal Ministry of Education and Science (BMBF 01ER0803 to C.S.), the Kommission für Klinische Forschung, Technische Universität München (KKF 8765162 to C.S), and a stipend of the Graduate school of Systemic Neurosciences (GSN LMU to A.M).

References

Arend, I., Rafal, R., Ward, R. 2008. Spatial and temporal deficits are regionally dissociable in patients with pulvinar lesions. Brain, 131(Pt 8) 2140-52.

Arnold, J. F., Zwiers, M. P., Fitzgerald, D. A., van Eijndhoven, P., Becker, E. S., Rinck, M., Fernandez, G., Speckens, A. E., & Tendolkar, I. 2012. Fronto-limbic microstructure and structural connectivity in remission from major depression. Psychiatry Res, 204(1), 40-48.

Awh, E. & Jonides, J., 2001. Overlapping mechanisms of attention and spatial working memory. Trends Cogn. Sci. 5, 119–126.

Beck, A.T., Steer, R.A., Brown, G.K., 1996. Manual for the Beck Depression Inventory-II. Second Edition ed. The Psychological Corporation, San Antonio, TX.

Bennaroch, E.E., 2015. Pulvinar: Associative role in cortical function and clinical correlations. Neurology, 84 (7), 738-747.

Behrens, T. E., Berg, H. J., Jbabdi, S., Rushworth, M. F., & Woolrich, M. W. 2007. Probabilistic diffusion tractography with multiple fibre orientations: What can we gain? Neuroimage, 34(1), 144-155.

Behrens, T. E., Johansen-Berg, H., Woolrich, M. W., Smith, S. M., Wheeler-Kingshott, C. A., Boulby, P. A., Barker, G. J., Sillery, E. L., Sheehan, K., Ciccarelli, O., Thompson, A. J., Brady, J. M., & Matthews, P. M. 2003. Non-invasive mapping of connections between human thalamus and cortex using diffusion imaging. Nat Neurosci, 6(7), 750-757.

Brown, E.C., Clark, D.,L., Hassel, D.S., MacQueen, G., Ramasubbu, R., 2017. Thalamocortical connectivity in major depressive disorder. J Affect Disord., 217, 125-131.

Buchsbaum, M.S., Buchsbaum, B.R., Chokron, S., Tang, C., Wei, T.C., Byne, W., 2006.Thalamocortical circuits: fMRI assessment of the pulvinar and medial dorsal nucleus in normal volunteers. Neurosci Lett., 404, 282–287.

Bundesen, C., 1990. A theory of visual attention. Psychol. Rev. 97, 523-547.

Bundesen, C., Habekost, T., Kyllingsbaek, S., 2005. A neural theory of visual attention: bridging cognition and neurophysiology. Psychol. Rev., 112, 291-328.

Chechlacz, M., Gillebert, C.R., Vangkilde, S.A., Petersen, A., Humphreys, G.W., 2015. Structural Variability within Frontoparietal Networks and Individual Differences in Attentional Functions: An Approach Using the Theory of Visual Attention. J. Neurosci., 35 (30), 10647-58.

Cieslik, E. C., Mueller, V. I., Eickhoff, C. R., Langner, R., & Eickhoff, S. B., 2015. Three key regions for supervisory attentional control: evidence from neuroimaging meta-analyses. Neuroscience & Biobehavioral reviews, 48, 22-34.

Corbetta, M., Miezin, F.M., Dobmeyer, S., Shulman, G.L., Petersen, S.E., 1991. Selective and divided attention during visual discriminations of shape, color, and speed: Functional anatomy by positron emission tomography. J Neurosci, 11, 2383–2402.

Cowan, N., 2001. The magical number 4 in short-term memory: a reconsideration of mental storage capacity. Behav. Brain. Sci. 24, 87-114.

Danziger, S., Ward, R.,, Owen, V.,, Rafal, R., 2001-2002.The effects of unilateral pulvinar damage in humans on reflexive orienting and filtering of irrelevant information. Behav. Neurol., 13, 95-104

Danziger, S., Ward, R., Owen, V., Rafal, R., 2004. Contributions of the human pulvinar to linking vision and action. Cogn Affect Behav Neurosci. 4(1), 89-99.

Desseilles, M., Schwartz, S., Dang-Vu, T.T., Sterpenich, V., Ansseau, M., Maquet, P., Phillips, C., 2011. Depression alters "top-down" visual attention: a dynamic causal modeling comparison between depressed and healthy subjects. Neuroimage, 54(2), 1662-8.

Desimone, R., & Duncan, C., 1995. Neural mechanisms of selective visual attention. Annu. Rev. Neurosci. 18, 193-222.

Desimone, R., & Ungerleider, L. G.,1989. Neural Mechanisms of Visual Processing in Monkeys, eds. Boller, F. & Grafman, 14, 267–299.

Donahue, C.J., Sotiropoulos, S.N., Jbabdi, S., Hernandez-Fernandez, M., Behrens, T.E., Dyrby, T., Coalson, T., Kennedy, H., Knoblauch, H., Van Essen, D.C., Glasser. M.F. 2016. Using Diffusion Tractography to Predict Cortical Connection Strength and Distance: A Quantitative Comparison with Tracers in the Monkey. J. Neurosci., 36 (25), 6758-6770.

Elliott, R., Dolan, R.J., 1998. Activation of different anterior cingulate foci in association with hypothesis testing and response selection. Neuroimage, 8, 17–29.

Espeseth, T., Vangkilde, S.A., Petersen, A., Dyrholm, M., Westlye, L.T., 2014. TVA-based assessment of attentional capacities-associations with age and indices of brain white matter microstructure. Front. Psychol. 5, 1177.

Fassbender, C., Murphy, K., Hester, R., Meaney, J., Robertson, I.H., Garavan, H., 2006. The role of a right fronto-parietal network in cognitive control: common activations for “cues-to-attend” and response inhibition. Journal of Psychophysiology, 20, 286–296.

Fisher, J., & Whitney, D., 2012. Attention gates visual coding in the human pulvinar. Nature Communications, 3:1051.

Finke, K., Bublak, P., Krummenacher, J., Kyllingsbæk, S., Müller, H.J., Schneider, W.X., 2005. Usability of a theory of visual attention (TVA) for parameter-based measurement of attention I: evidence from normal subjects. J. Int.Neuropsychol.Soc. 11, 832–842.

Finke, K., Bublak, P., & Zihl, J., 2006. Visual spatial and visual pattern working memory: Neuropsychological evidence for a differential role of left and right dorsal visual brain. Neuropsychologia, 44(4), 649-661.

Garavan, H., T. J. Ross, and E. A. Stein., 1999. Right hemispheric dominance of inhibitory control: an event-related functional MRI study. Proceedings of the National Academy of Sciences, 96(14), 8301-8306.

Golestani, A.M., Miles, L., Babb, J., Castellanos, F.X., Malaspina, D., Lazar, M., 2014. Constrained by Our Connections: White Matter's Key Role in Interindividual Variability in Visual Working Memory Capacity. J. Neurosci. 34 (45), 14913-14918.

Habekost, T., Petersen, A., Vangkilde, S., 2014.Testingattention:comparing the ANT with TVA-based assessment. Behav.Res.Methods 46, 81–94.

Habekost, T. (2015). Clinical TVA-based studies: a general review. Frontiers in psychology, 6, 290.

Habekost, T., & Rostrup, E. 2006. Persisting asymmetries of vision after right side lesions. Neuropsychologia, 44(6), 876-895.

Habekost, T., Rostrup, E., 2007. Visual attention capacity after right hemisphere lesions. Neuropsychologia 45, 1474-1488.

Halassa, M.M., Kastner, S., 2017.Thalamic functions in distributed cognitive control. Nature Neuroscience, 20, 1669-1679.

Hampshire, A., Chamberlain, S. R., Monti, M. M., Duncan, J., & Owen, A. M. (2010). The role of the right inferior frontal gyrus: inhibition and attentional control. Neuroimage, *50*(3), 1313-1319.

Hebb, D. O., 1949. Organization of behavior. New York: Wiley

Jbabdi, S., & Johansen-Berg, H. (2011). Tractography: where do we go from here? Brain Connect, 1(3), 169-183

Jbabdi, S., Sotiropoulos, S.N., Haber, S.N., Van Essen, D.C., Behrens, T.E. 2015. Measuring macroscopic brain connections in vivo. Nat Neurosci. 18(11), 1546-55.

Jenkinson, M., Beckmann, C. F., Behrens, T. E., Woolrich, M. W., & Smith, S. M. (2012). FSL. Neuroimage, 62(2), 782-790.

Jeurissen, B., Descoteaux, M., Mori, S., Leemans, A., 2017. Diffusion MRI fiber tractography of the brain. NMR Biomed.

Jones, D.K., 2010. Challenges and limitations of quantifying connectivity in the human brain in vivo with diffusion MRI. Imaging Med., 2, 341-355

Jones, D.K.**,** Knosche, T.R., Turner, R., 2013. White matter integrity, fiber count, and other fallacies: the do's and don'ts of diffusion MRI. Neuroimage, 73, 239-54.

Kraft, A., Irlbacher ,K., Finke, K., Kaufmann, C., Kehrer, S., Liebermann, D., Bundesen, C., Brandt, S.A., 2015. Dissociable spatial and non-spatial attentional deficits after circumscribed thalamic stroke. Cortex, 64, 327–342.

LaBerge, D., Buchsbaum, M.S., 1990. Positron emission tomographic measurements of pulvinar activity during an attention task. J Neurosci, 10, 613–619.

Lehr, S., 1977. Mehrfachwahl-Wortschatz-Intelligenztest MWT-B. Manual. Straube-Verlag, Erlangen.

Luck, S.J., Vogel, E.K., 1997. The capacity of visual working memory for features and conjunctions. Nature, 390, 279–281.

Malone, I.B., Leung, K.K., Clegg, S., Barnes, J., Whitwell, J.L., Ashburner, J., Fox, N.C., Ridgway, G.R., 2015. Accurate automatic estimation of total intracranial volume: a nuisance variable with less nuisance. Neuroimage, 104, 366-72.

Menegaux, A., Meng, C., Neitzel, J., Bauml, J. G., Muller, H. J., Bartmann, P., Wolke, D., Wohlschläger, A.M., 2017. Impaired visual short-term memory capacity is distinctively associated with structural connectivity of the posterior thalamic radiation and the splenium of the corpus callosum in preterm-born adults. Neuroimage, 150, 68–76.

Meng, C., Bäuml, J.G., Daamen, M., Jaekel, J., Neitzel, J., Scheef, L., Busch, B., Baumann, N., Boecker, H., Zimmer, C., Bartmann, P., Wolke, D., Wohlschläger, A.M., Sorg, C., 2015. Extensive and interrelated subcortical white and gray matter alterations in preterm-born adults. Brain Struct Funct 221 (4), 2109-21.

Nobre, A.C., Sebestyen, G.N., Gitelman, D.R., Frith, C.D., Mesulam, M.M., 2002. Filtering of distractors during visual search studied by positron emission tomography. NeuroImage, 16, 968–976.

Okon-Singer, H., Podlipsky, I., Siman-Tov, T., Bin-Simon, E., Zhdanov, A., Neufeld, M.Y., Hendler, T. 2011. Spatio-temporal indications of sub-cortical involvement in leftward bias of spatial attention. NeuroImage, 54(4), 3010-3020.

Oldfield, R.C., 1971. The assessment and analysis of handedness: the Edinburgh inventory. Neuropsychologia. 9(1), 97-113.

Reveley, C., Seth, A.K., Pierpaoli, C., Silva, A.C., Yu, D., Saunders, R.C., Leopold, D.A., Ye, F.Q., 2015. Superficial white matter fiber systems impede detection of long-range cortical connections in diffusion MR tractography. Proc Natl Acad Sci U S A, 112, 2820–2828.

Rilling, J.K., Glasser, M.F., Preuss, T.M., 2008. The evolution of the arcuate fasciculus revealed with comparative DTI. Nat. Neurosci., 11(4), 426–428.

Rorden, C., Karnath, H.O., Bonilha, L., 2007. Improving lesion-symptom mapping. J. Cog. Neurosci., 19(7), 1081-8.

Saalmann, Y.B., Pinsk, M.A., Wang, L., Li X., Kastner S., 2012. The pulvinar regulates information transmission between cortical areas based on attention demands. Science, 337, 753-756.

Shipp, S., 2003. The functional logic of cortico-pulvinar connections. Philos. Trans. R. Soc. Lond. B Biol. Sci., 358,1605-1624.

Shipp, S., 2004. The brain circuitry of attention.Trends Cogn. Sci., 8, 223-23**Snow,** J.C., Allen, H.A., Rafal, R.D., Humphreys, G.D., 2009. Impaired attentional selection following lesions to human pulvinar: evidence for homology between human and monkey. Proc. Natl. Acad. Sci. USA, 106, 4054-4059.

Smith, E. E., Jonides, J., Koeppe, R.A., Awh, E., 1995. Spatial versus object working memory: PET investigations. J. Cogn. Neurosci. **7**, 337–358.

Snow, J.C., Allen, H.A., Rafal, R.D., Humphreys, G.W., 2009. Impaired attentional selection following lesions to human pulvinar: evidence for homology between human and monkey. Proc Natl Acad Sci U S A., 106, 4054–4059.

Strumpf, H., Mangun, G.R., Boehler, C.N., Stoppel, C., Schoenfeld, M.A., Heinze, H.J., Hopf, J.M., 2013 Hum Brain Mapp., 34(5), 1115-32.

Thomas, C., Ye, F.Q., Irfanoglu, M.O., Modi, P., Saleem, K.S., Leopold, D.A., Pierpaoli, C., 2014. Anatomical accuracy of brain connections derived from diffusion MRI tractography is inherently limited. Proc Natl Acad Sci U S A, 111,16574–16579.

Todd, J. J., & Marois, R., 2005. Posterior parietal cortex activity predicts individual differences in visual short-term memory capacity. Cognitive, Affective, & Behavioral Neuroscience, 5(2), 144-155.

Tuch, D.S., Reese, T.G., Wiegell, M.R., Makris, N., Belliveau, J.W., Wedeen, V.J., 2002. High angular resolution diffusion imaging reveals intravoxel white matter fibre heterogeneity. Magn. Reson. Med. 48, 577–582.

Tuch, D.S., Reese, T.G., Wiegell, M.R., Wedeen, V..J., 2003. Diffusion MRI of complex neural architecture. Neuron. 40, 885–895.

Verleger, R., Sprenger, A., Gebauer, S., Fritzmannova, M., Friedrich, M., Kraft, S., & Jaśkowski, P. 2009. On why left events are the right ones: Neural mechanisms underlying the left-hemifield advantage in rapid serial visual presentation. Journal of cognitive neuroscience, 21(3), 474-488.

Vogel, E.K., Machizawa, M.G., 2004. Neural activity predicts individual differences in visual working memory capacity. Nature, 428,748–751

Vos S.B., Jones, D.K., Viergever, M.A., Leemans, A., 2011. Partial volume effect as a hidden covariate in DTI analyses. Neuroimage. 55(4), 1566-76.

Wurtz, R.H., Joiner, W.M., Berman, R.A., 2011. Neuronal mechanisms for visual stability: progress and problems. Philos Trans R Soc Lond B Biol Sci.,366(1564),492-503.

Zhang, D., Snyder, A. Z., Shimony, J. S., Fox, M. D., & Raichle, M. E. 2010. Noninvasive functional and structural connectivity mapping of the human thalamocortical system. Cereb Cortex, 20(5), 1187-1194.

Zhou, H., Schafer, R.J., Desimone R.,2016. Pulvinar-Cortex Interactions in Vision and Attention. Neuron, 89(5), 209-220.

Supplementary material

Figure S1: Inter-individual variability of thalamic probability maps.

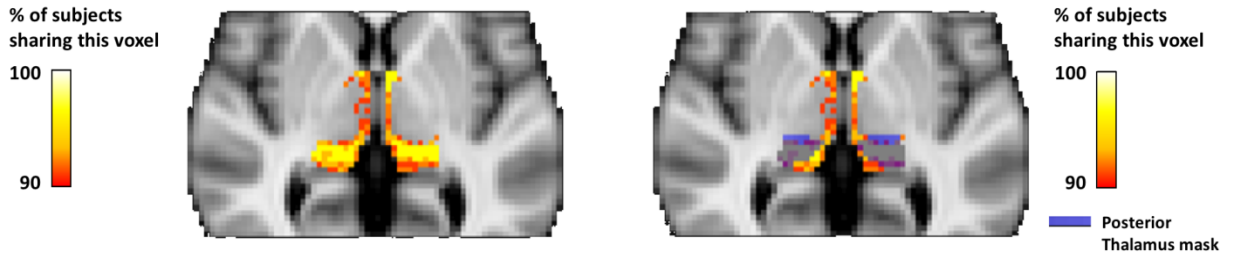

Figure S1: Yellow and orange colors represent voxels that are present in at least 90% of the participants; blue illustrates bilateral posterior thalamus mask.

Table S1: Comparison of K and C parameters for t_0<0 correction vs original value

	t_0<0 set to 0		t_0<0 unchanged	
	M	*SD*	*M*	*SD*
K	3.306	0.392	3.310	0.397
C	24.733	8.661	24.361	8.436

Table S2: Correlation between K and C parameters and posterior thalamus structural connectivity for original t_0<0 values

		Left PT-OC SC	Right PT-OC SC	Left PT-MC SC	Right PT-MC SC
K	t_0<0 unchanged	**r = -0.38 p = .03***	r = 0.02 p = .91	r = 0.02 p = .90	r = -0.10 p = .60
C	t_0<0 unchanged	r = -0.19 p = .29	r = 0.08 p = .67	r = 0.12 p = .51	r = -0.01 p = .95

Abbreviations: PT-OC: Posterior thalamus to occipital cortex; PT-MC: Posterior thalamus to motor cortex; SC structural connectivity. Correlations below p = .10 are shown in bold, * indicates a p < .05.

Table S3: Coefficients of multiple linear regression for vSTM capacity and left PT-OC connection probability

	Dependent variable = vSTM capacity		
Independent variables	**ß values**	**P value**	**95% CI**
Left PT-OC connection probability	**-26.823**	**.008**	[-46.206 , -7.440]
Age	-.006	.304	[-.019 , .006]
Gender	-.038	.781	[-.317 , .241]
Handedness	-.227	.121	[-.519 , .064]
TIV	-.540	.465	[-2.030 , .949]
IQ	**0.10**	**.017**	[.002 , .018]

Table S4: Coefficients of multiple linear regression for vSTM capacity and right PT-OC connection probability

	Dependent variable = vSTM capacity		
Independent variables	**ß values**	**P value**	**95% CI**
Right PT-OC connection probability	3.605	.775	[-21.965 , 29.176]
Age	-.009	.202	[-.023 , .005]
Gender	-.038	.806	[-.353 , .276]
Handedness	-.142	.384	[-.469 , .188]
TIV	.144	.855	[-1.460 , 1.748]
IQ	**0.11**	**.023**	[.002 , .020]

Table S5: Coefficients of multiple linear regression for top-down control and left PT-OC connection probability

	Dependent variable = Top-down control		
Independent variables	**ß values**	**P value**	**95% CI**
Left PT-OC connection probability	-1.232	.752	[-9.135 , 6.671]
Age	.004	.121	[-.001 , .009]
Gender	.102	.077	[-.012 , .216]
Handedness	.064	.280	[-.055 , .183]
TIV	.047	.125	[-1.077 , .137]
IQ	-.001	.674	[-.004 , .003]

Table S6: Coefficients of multiple linear regression for top-down control and left PT-OC connection probability

	Dependent variable = Top-down control		
Independent variables	**ß values**	**P value**	**95% CI**
Right PT-OC connection probability	**8.854**	**.046**	[.166 , 17.541]
Age	.003	.144	[-.001 , .008]
Gender	.111	.043	[.004 , .217]
Handedness	.089	.111	[-.022 , .200]
TIV	-.362	.185	[-.907 , .183]
IQ	-.001	.550	[-.004 , .002]

Table S7: Correlation table between tract lateralization index and parameters vSTM capacity and top-down control

	Tract Lateralization Index
K	**r = -0.36 p = .042***
α	**r = -0.35 p = .047***